Journal of proteome research

Article

Cite This: J. Proteome Res. 2018, 17, 3791−3800

pubs.acs.org/jpr

# Increasing the Separation Capacity of Intact Histone Proteoforms Chromatography Coupling Online Weak Cation Exchange-HILIC to Reversed Phase LC UVPD-HRMS

Andrea F. G. Gargano,*[,†,‡] Jared B. Shaw,[§] Mowei Zhou,[§] Christopher S. Wilkins,[∥] Thomas L. Fillmore,[∥] Ronald J. Moore,[∥] Govert W. Somsen,[†,‡] and Ljiljana Paša-Tolić[§]

[†]Center for Analytical Sciences Amsterdam, Science Park 904, 1098 XH Amsterdam, The Netherlands

[‡]Vrije Universiteit Amsterdam, Department of Bioanalytical Chemistry, Amsterdam Institute for Molecules, Medicines and Systems, de Boelelaan 1085, 1081HV Amsterdam, The Netherlands

[§]Environmental Molecular Sciences Laboratory, Pacific Northwest National Laboratory, P.O. Box 999, Richland, Washington 99352, United States

[∥]Biological Sciences Division, Pacific Northwest National Laboratory, P.O. Box 999, Richland, Washington 99352, United States

Supporting Information

**ABSTRACT:** Top-down proteomics is an emerging analytical strategy to characterize combinatorial protein post-translational modifications (PTMs). However, sample complexity and small mass differences between chemically closely related proteoforms often limit the resolution attainable by separations employing a single liquid chromatographic (LC) principle. In particular, for ultramodified proteins like histones, extensive and time-consuming fractionation is needed to achieve deep proteoform coverage. Herein, we present the first online nanoflow comprehensive two-dimensional liquid chromatography (nLC×LC) platform top-down mass spectrometry analysis of histone proteoforms. The described two-dimensional LC system combines weak cation exchange chromatography under hydrophilic interaction LC conditions (i.e., charge- and hydrophilicity-based separation) with reversed phase liquid chromatography (i.e., hydrophobicity-based separation). The two independent chemical selectivities were run at nanoflows (300 nL/min) and coupled online with high-resolution mass spectrometry employing ultraviolet photodissociation (UVPD-HRMS). The nLC×LC workflow increased the number of intact protein masses observable relative to one-dimensional approaches and allowed characterization of hundreds of proteoforms starting from limited sample quantities (∼1.5 μg).

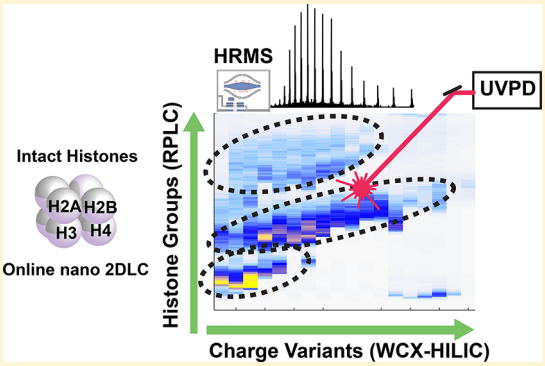


**KEYWORDS:** *histones, top-down mass spectrometry, online comprehensive two-dimensional liquid chromatography, ultraviolet photodissociation, post-translational modifications*

## INTRODUCTION

Histones are highly heterogeneous chromatin proteins with an isoelectric point of ∼11 and a molecular mass of 10−22 kDa. The histone octamer is composed of two H2A, H2B, H3, and H4 proteins assembled as one H3−H4 heterotetramer and two H2A-H2B heterodimers, with roughly 147 bp of DNA wrapped around it.[1] This protein−DNA complex is the basic structural unit of chromatin, the nucleosome. Post-translational modifications (PTMs) of histones have defined roles in regulating gene transcription.[2−4] For instance, increased acetylation is typically associated with gene activation due to a more open chromatin structure that makes it accessible to transcription factors. Another example is methylation, which can be associated with either transcriptional repression or activation, depending on the site and degree of methylation.[1−3]

Traditionally, histone samples are studied using antibody-based enrichment methods.[5] However, immunoprecipitation methods are unable to identify novel PTMs, as they require previous knowledge of the type of modification and a highly specific antibody for each modification studied. Moreover, many antibodies are not entirely site specific and can cross-react with similar modifications on different residues.[6]

Mass spectrometry (MS) based analyses of histone PTMs have emerged as an attractive alternative to traditional antibody-based methods.[7−12] Bottom-up methods, employing protein digestion prior to liquid chromatography (LC)-MS analysis, are established approaches to characterize proteins and their PTMs. However, a limitation of these strategies is

Received: June 14, 2018
Published: September 18, 2018




DOI: 10.1021/acs.jproteome.8b00458
J. Proteome Res. 2018, 17, 3791−3800

their inability to assign a specific modified peptide sequence to a particular proteoform.[13] Histones, in particular, are rich in lysine and arginine, and bottom-up methods using trypsin cleave histones into peptides that are too short for effective LC-MS analysis. Additionally, connectivity between peptides is lost making it impossible to retrieve exact proteoforms.[10,14] Middle-down methods performed using enzymes with rare cleavage sites or chemically blocking unmodified lysine can generate large peptides (about 30−60 amino acid residues). Analysis of longer peptides enables identification of combinatorial PTMs and the crosstalk between PTMs.[10,15,16] However, characterization of proteins like histones H2B requires analysis of the intact protein due to variants that differ by one or a few amino acids near both the N- and C-termini. Complete characterization of the combinatorial distribution of histone proteoforms is only possible via the analysis of intact histones using top-down proteomic approaches.[17−19] Quantitative analysis of proteoforms of isolated histone H4[20] and H2A and H2B[21] have been recently reported demonstrating the applicability of such workflows to biological studies. However, despite recent improvements in instrumentation and methodology, top-down analyses still face many practical challenges in sample preparation, separations, MS detection, and informatics.[22]

For histones, isolation of nuclei from other cellular contents is usually preferred to obtain sufficiently pure histones for in-depth PTM profiling. However, the yield of nuclei isolation and histone extraction can vary significantly across organisms and cell types, limiting the amount of histone proteins available for LC-MS analysis. Even for global top-down analyses, sample prefractionation is typically needed to enable comprehensive coverage of the various proteoforms. Therefore, advanced LC methods that offer a streamlined purification and fractionation process would be highly beneficial.

The two most commonly used separation methods in the top-down analysis of histones are weak cation exchange-hydrophilic interaction liquid chromatography (WCX-HILIC) and reversed phase liquid chromatography (RPLC). The ion exchange nature of WCX-HILIC makes this separation method selective toward histone charge variants (e.g., resulting from lysine acetylation).[23] However, WCX-HILIC has low MS compatibility and limited separation efficiency. RPLC provides good MS compatibility but has limited proteoform selectivity and primarily resolves the main histone families (H1, H2A, H2B, H3, and H4).[24]

Here we present an online nanoflow LC×LC method that enables comprehensive characterization of histone proteoforms. The 2DLC setup couples a WCX-HILIC using a shallow gradient in the first dimension to a fast RPLC in the second separation dimension. The two liquid phase separations are coupled using a modulation interface having trap columns (active modulation, a×m) allowing both separations to run at a flow rate of 300 nL/min. Our separation setup was coupled to a Q Exactive HF Orbitrap mass spectrometer modified to incorporate 193 nm ultraviolet photodissociation (UVPD).[25−27]

By combining the WCX-HILIC/a×m/RPLC with UVPD-HRMS, we were able to identify hundreds of HeLa core histone proteoforms using a small amount of starting material (~1.5 μg). These results suggest that 2DLC-MS platforms could significantly improve our ability to analyze proteoforms present in biologically relevant samples available in limited amounts (e.g., derived from laser microdissection).

## EXPERIMENTAL SECTION

### Chemicals and Reagents

Formic acid (FA), ammonium formate, and ammonium acetate were purchased from Sigma-Aldrich. The solvents used were Milli-Q grade water (18.2 mΩ) and mass spectrometry grade acetonitrile (ACN). HeLa core histones were purchased from ActiveMotif (Carlsbad, CA). The sample was buffer exchanged into water using 3 kDa molecular weight cutoff filters (EMD Millipore, Billerica, MA) and stored at −70 °C. We prepared a histone sample for WCX-HILIC and HILIC/a×m/RPLC analysis as a 0.52 μg/μL solution in 50/50 ACN/5 mM ammonium acetate (v/v). Samples for RPLC were prepared in the same concentration but dissolved in 2% ACN 0.1%FA. All the columns and trap columns used in this study were packed in-house.

### 1DLC Analysis (WCX-HILIC and RPLC Analysis)

One dimensional LC analyses (1DLC) were done using a Waters M-Class LC operated using MassLynx. The WCX-HILIC separation method was developed based on workflow described by Tian et al.[28] The chromatographic column used was a silica based weak cation exchanger (PolyCAT A, 5 μm particles, 1000 Å pore size; Poly LC, Columbia, MD, USA) packed in a 150 mm × 75 μm I.D. column. The optimized method used 70/29/1 ACN/water/FA as mobile phase A and 65/27/8 ACN/water/FA (v/v/v) as mobile phase B. The analyses were done at 300 nL/min using a gradient from 0% B to 100% B in 100 min, 20 min at 100% B, and with 30 min of equilibration at 0% after each injection. Injections were done using a 5 μL loop in partial injection mode (solvent, 90/10 ACN/10 mM ammonium acetate).

We performed the 1D RPLC separation on a 700 mm long 75 μm ID column packed with C18 silica (Jupiter C18, 3 μm particles, 300 Å pore size, Phenomenex, Torrance, CA, USA). We used 0.1% FA in water as mobile phase A and 0.1% FA in ACN as B. The sample was injected using a 20 μL loop in full loop mode and trapped on a C18 trap column (Phenomenex Aeris XB-C18, 3.6 μm particles, 200 Å pore size, 50 mm × 100 μm). The sample was desalted on the trap cartridge for 20 min at 5% solvent B at a flow rate of 2.5 μL/min. Subsequently, the flow was reduced to 0.3 μL/min and directed to the C18 column. For elution we used a linear gradient starting at 10% solvent B and increasing to 20% B in 5 min, and ramped to 50% B at 100 min then to 80% B in 10 min and washing the column for 20 min at 80% B and then re-equilibrated at 5% B for 20 min.

### Online Comprehensive Two-Dimensional LC (WCX-HILIC/a×m/RPLC, 2DLC)

The two-dimensional separation platform was assembled from Waters M-Class LC modules (2 gradient-pumps, one used as gradient pump for the $^{2}$D column and one for delivering the dilution flow; autosampler with 5 μL loop installed), one Acquity NanoLC pump (gradient pump used for the $^{1}$D column), and a nanoswitching valve from VICI Valco (PN C72MX-6670D 10-ports two-positions). We chose to use this valve because of the reduced port to port valve volume (approximately 30 nL). A schematic diagram of the 2DLC system is shown in Figure 2. We used two computers running MassLynx to control the online 2DLC system, one unit (PC1) controlling the first-dimension pump ($^{1}$D) and one (PC2) controlling the autosampler (connected to the $^{1}$D column, WCX-HILIC), second dimension pump ($^{2}$D), and the



DOI: 10.1021/acs.jproteome.8b00458
J. Proteome Res. 2018, 17, 3791−3800

**Table 1. Histone Proteoforms Identified by the Injection of 1.5 μg of HeLa Core Histones into the RPLC, WCX-HILIC, or WCX-HILIC/axm/RPLC Coupled with UVPD-HRMS[a]**

| LC-MS method | H2A | H2B | H3 | H4 | Total unique ID |
|---|---|---|---|---|---|
| 1DLC RPLC–UVPD-MS[b] | 19 (42) | 12 (23) | 36 (59) | 16 (39) | 83 (163) |
| 1DLC WCX-HILIC–UVPD-MS[b] | 6 (7) | 10 (10) | 173 (177) | 19 (21) | 208 (215) |
| 2DLC WCX-HILIC/a×m/RPLC-UVPD-MS R1[c] | 26 (29) | 12 (14) | 299 (299) | 29 (37) | 366 (379) |
| 2DLC WCX-HILIC/a×m/RPLC-UVPD-MS R2[c] | 33 (39) | 14 (16) | 293 (298) | 21 (30) | 361 (383) |
| 2DLC WCX-HILIC/a×m/RPLC-UVPD-MS R3[c] | 30 (33) | 13 (16) | 327 (338) | 21 (25) | 391 (412) |

[a]The identifications are obtained from searches against histone and contaminants database using Prosight PC (see Experimental Section for details). The data in parentheses indicate the total number of identifications, including the one from truncated forms (absolute and biomarker data search). Data filtered for $P < 1E^{-4}$. Protein IDs available in Table S3 of the Supporting Information. [b]150 min acquisition time. [c]270 min acquisition time.

switching valve. The two LC dimensions and MS were synchronized using contact closure relays.

For the first LC separation, we used the same column described for the WCX-HILIC separation. The second-dimension column was packed in a 100 mm × 50 μm ID column, using reversed phase material (Jupiter C18, 3 μm particles, 300 Å pore size, Phenomenex, Torrance, CA, USA). Trap columns were prepared in a 50 mm × 100 μm ID columns using C18 core–shell particles (Aeris C18, 3.6 μm particles, 200 Å pore size, Phenomenex, Torrance, CA, USA).

We used mobile phase A1 70/29/1 ACN/water/FA and mobile phase B1 65/27/8 ACN/water/FA (v/v/v) for $^1$D. $^2$D used mobile phase A2 (0.1% FA in water) and B2 (0.1% FA in ACN). We applied gradient elution in both dimensions.

A constant flow of 1.6 μL/min of 1% ACN 0.1% TFA (dilution flow) was pumped via a tee union (VICI-Valco, C360QTPK2) connecting to the WCX-HILIC column and the modulation interface.

To complete the elution in the $^1$D and reduce carry over between analyses, we programmed the autosampler to perform full loop injection (5 μL plugs) from vials containing mobile phases with increasing water content (the solvent compositions are reported below) at the end of the $^1$D gradient.

PC2 triggered both the LC and MS run via the second pump module ($^2$D) and was responsible for the injection on the WCX-HILIC column ($^1$D). The $^2$D separations were programmed as a sequence of runs. We programmed the sequence of $^2$D separations with the first method injecting the sample, followed by 13 injections where no sample nor solvent was injected ("blank" injection), 5 analyses (15th, 16th, 17th, 18th and 19th $^2$D) where 5 μL of, respectively, 65/8/27, 60/8/32, 50/8/42, 25/8/67, 5/8/87 ACN/FA/water were injected, and a last $^2$D method (20th) where no sample nor solvent was injected. The total analysis time per run was 275 min.

## Mass Spectrometry and Ultraviolet Photodissociation

Both the 1DLC configurations (WCX-HILIC and RPLC) as well as the WCX-HILIC/a×m/RPLC setup were coupled via a nanoelectrospray (ESI) source to a Q Exactive HF mass spectrometer (ThermoFisher Scientific Inc.) modified in a similar fashion as previously described to enable UVPD in the HCD cell.[29] The ESI voltage was set at 1.6 kV, with the inlet capillary temperature at 270 °C and S-RF lens at 70%. All the experiments were performed at a nominal resolving power of 120 000 ($m/z$ = 200) for MS1 and 60 000 for MS/MS experiments. MS and MS/MS automatic gain control (AGC) target values were set at 3e6 (50 ms as maximum injection time) and 5e5 (200 ms), respectively. The number of microscans for MS1 and MS/MS was 3 and 6, respectively. The MS data were acquired as profile data, for 500 < $m/z$ < 2000. Data dependent top 5 acquisitions (AGC minimum 2e4, intensity threshold 1e5) were performed with a 2 Th isolation window followed by UVPD using a single 1 mJ pulse. Dynamic exclusion was implemented with an exclusion duration of 60 s. MS/MS was only performed on species with charge states greater than four.

## Data Analysis

Data analysis was performed using ProSightPC 4.0 (ThermoFisher Inc.) and Informed Proteomics (https://github.com/PNNL-Comp-Mass-Spec/Informed-Proteomics).[30] Prosight PC 4.0 was used to generate the results reported in Tables 1 and 2, and Informed Proteomics was used as a visualization and confirmatory tool to annotate the IDs (examples of protein identifications are collected in Supporting Materials S6 and S7).

**Table 2. Unique Histone Proteoforms Identified Using ProSight Absolute Mass Search against the Human Proteome[a]**

| LC-MS method | $C < 3$ | $3 \le C \le 45$ | $C > 45$ | Total Unique IDs with $C > 3$ (total IDs) |
|---|---|---|---|---|
| 1DLC RPLC–UVPD-MS | 147 | 51 | 16 | 67 (155) |
| 1DLC WCX-HILIC–UVPD-MS | 108 | 29 | 8 | 37 (128) |
| 2DLC WCX-HILIC/a×m/RPLC-UVPD-MS R1 | 158 | 61 | 28 | 87 (173) |
| 2DLC WCX-HILIC/a×m/RPLC-UVPD-MS R2 | 175 | 62 | 30 | 92 (189) |
| 2DLCWCX-HILIC/a×m/RPLC-UVPD-MS R3 | 173 | 61 | 31 | 92 (190) |

[a]Identifications are sorted according to their $C$ score. The total number of identified proteoforms is given in parentheses. Data filtered for $P < 1E^{-4}$. Protein IDs available in Table S4 of the Supporting Information.

Two search modes of ProSight PC were used: absolute mass search to identify full-length proteins and biomarker search to identify protein fragments. Absolute mass search restricts the search space to proteins matching the mass of the precursor, whereas, in biomarker search, the search space is extended to protein sequence fragments matching the mass of the precursor. The data analysis was about 2 days per data set when performing absolute mass and biomarker searches in Prosight PC.



DOI: 10.1021/acs.jproteome.8b00458
J. Proteome Res. 2018, 17, 3791–3800

Alternatively, we created a database containing all histone proteins and common protein contaminants found in our samples (62 proteins). The restricted protein list was created from searches using Prosight PC performing absolute mass searches against the complete Human proteome using 1D (RPLC and WCX) and 2DLC-HRMS data allowing for 5 PTMs and 10 ppm mass accuracy for matching parent ions and fragment ions (reported in Table S2 of the Supporting Information). The database was created allowing for a maximum of 13 PTMs per protein.

Table 1 lists proteins identified using Prosight PC 4.0 for searches against the confined database and applying UVPD fragmentation settings for top-down MS2. RAW files were processed using the Xtract algorithm and Top Down (MS2) default settings. The analysis was performed in Absolute mass mode with a mass tolerance of 10 ppm for precursor and 10 ppm for fragments using the Δm mode (this function allows identification of proteoforms with PTMs not included in the annotated proteoform database). The unmatched spectra were further searched in Biomarker discovery mode, using the same mass tolerance settings. Histone identifications were filtered using the best hit per experiment function and a $P < 1 \times 10^{-04}$ cutoff. Analysis of a single data set with this approach took 2 days on a personal computer with an Intel Core i7-3820 CPU processor at 3.6 GHz with 32 GB of RAM. Additionally, we searched all data sets against the "histone&contaminants database" using the Informed-Proteomics workflow:[30] ProMex software was used for intact mass deconvolution, MSPath-Finder was used as the search engine, and LcMsSpectator as data visualization tool. The feature maps reported in various figures were obtained using LcMsSpectator. The deconvolution and search settings were similar to the one in Prosight PC. MSPath-Finder does not use previous knowledge regarding the PTM site and type of modification (e.g., from uniprot.org). Our searches allowed for a maximum of 5 PTMs per protein and mono-, di-, and trimethylation, acetylation, and phosphorylation.

The results reported in Table 2 were generated from ProsightPC using absolute mass searches against the complete human proteome, with a mass tolerance of 10 ppm for the precursor and 10 ppm for fragments, allowing up to 13 PTMs (but removing the Δm search mode) and filtered using the $P < 1 \times 10^{-04}$ cutoff and according to C score results.[31]

The mass spectrometry data have been deposited to the PRIDE Archive (http://www.ebi.ac.uk/pride/archive/) via the PRIDE partner repository with the data set identifier PXD008978.

## RESULTS AND DISCUSSION

### Top Down Analysis of Histones by 1DLC-MS

Weak cation exchange LC (WCX) separations using poly(aspartic acid) functionalized silica materials and mobile phases rich in ACN (e.g., 70% ACN) have been used to study the distribution of intact[23,28,32,33] and "partially digested" (middle down) proteoforms of histones.[16,34−36] The combination of ion exchange and hydrophilic interactions makes these separations selective toward PTMs that modify the charge of the protein (e.g., lysine acetylation). However, in order to ensure the complete elution of these basic proteins, typical separation methods are performed using high acid (e.g., 8% to 10% FA) or salt (e.g., 1 M $NaClO_4$) concentration, hindering in some cases the direct coupling of WCX-HILIC with MS. Coupling to MS is possible using volatile additives. However, their high concentration can cause ion suppression and/or ESI instability, requiring frequent cleaning of the ion source, thus making the WCX-HILIC technique nonideal for high-throughput analyses.

Despite these drawbacks, WCX-HILIC offers excellent resolving power for acetylated and methylated species.[32,33,37] Figure 1a shows total ion chromatogram and deconvoluted

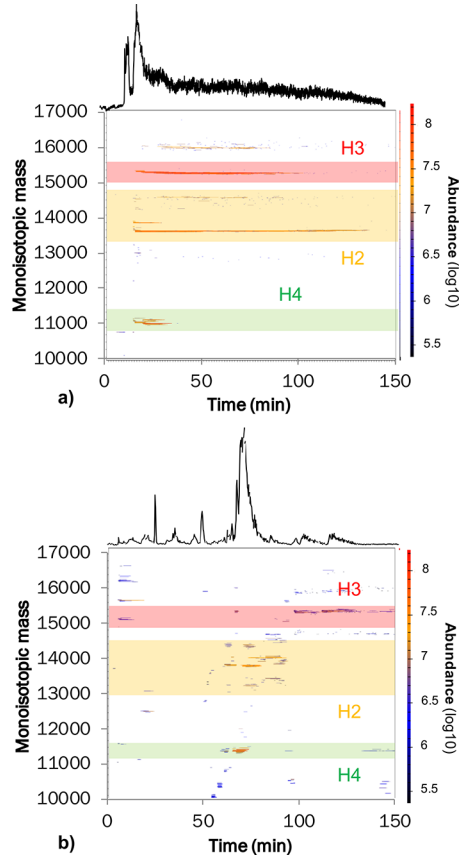


**Figure 1.** TIC LC-MS chromatogram (top) and feature map (deconvoluted mass spectra vs time) LC-MS chromatograms of 1DLC analysis (a) WCX-HILIC run and (b) RPLC MS. The colored areas indicate the elution zone of the different histone groups.

mass vs retention time (i.e., LC-MS feature map) reconstructed from the analysis of 1.5 μg of HeLa histones. In our experiments, gradients similar to the one described by Garcia et al.[16] (using 0.5% FA and 20% of ACN) were not entirely successful in eluting proteoforms of H3 histones with low amounts of acetylation and methylation. We therefore applied the strategy reported by Tian et al.[28] where a high concentration of formic acid enables more efficient elution of H3 histones.

The WCX-HILIC separation under the conditions described provides a continuous elution of histone proteins, where proteoforms with a higher degree of acetylation (thus higher mass) elute first, followed by the less modified proteoforms. Previous studies have described the retention mechanism for this separation, suggesting the acetylation of arginine or lysine residues as the main driving force for chemical discrimination.[28,35,38] Acetylation decreases the basicity of histones and thus weakens the electrostatic interaction with the stationary phase (polyaspartic acid). However, as can be seen


DOI: 10.1021/acs.jproteome.8b00458
J. Proteome Res. 2018, 17, 3791−3800

in Figure 1a almost no discrimination between histone families is possible using this separation approach. The LC-MS feature maps for each histone group are reported in Supporting Material S3.

Top-down MS studies of histones using RPLC are typically done employing water to ACN gradients in the presence of an acidic modifier and can be easily coupled to MS via ESI. Different types of stationary phases have been used to separate histone families (H1, H2, H3, and H4), including C4, C5, C8,[23,33,39−41] and C18 materials.[7,42,43] Figure 1b shows the LC−MS feature map obtained from the injection of 1.5 μg of HeLa core histones on a C18 RPLC column. With this separation, the major histone families are resolved into different regions based on their hydrophobicity (defined primarily by amino acid composition and mass). H4 and H2B elute early, followed by H2A, and finally H3 proteoforms elute over a broad retention time range.

WCX-HILIC and RPLC methods target different sample properties[44] (i.e., charge vs hydrophobicity), and their coupling in various arrangements has proven to increase the overall number of identified species relative to one-dimensional methods.[23,28,45] Although more informative, these analytical workflows are not common due to potential sample losses (inherent to offline fractionation) and long analysis time. Initial research using offline 2DLC workflows used up to 100−150 μg of purified histones proteins.[45] Miniaturized fractionation columns reduced the quantity of sample needed for offline configurations to 7.5 μg.[24] Although the sample consumption can be reduced by fractionating the sample using smaller column IDs, this does not help to reduce the overall analysis time. For instance, Tian et al.[28] described an offline 2DLC workflow for fractionation of 7.5 μg of purified histone by capillary RPLC followed by sequential WCX-HILIC analyses. Despite reducing the sample quantity, the overall analysis time was over 900 min. Such a long analysis time limits the practicality of this workflow for high-throughput applications

The only online 2DLC setup for the analysis of histone proteoforms described so far is the multiple heart-cut system reported by Tian et al.[23] In this setup, multiple loops were used to collect 20 fractions from a 300 min WCX-HILIC separation using nine switching valves, several trap columns, and two RPLC columns. This configuration demonstrated a significant increase in the number histone proteoform identifications but required a large sample quantity (24 μg) and long analysis time (more than 60 h for a single analysis) which significantly diminished its applicability. This inspired us to develop a nanoflow online 2DLC method that would combine the advantages provided by coupling independent separation modalities with a small sample requirement and shorter analysis time.

In comparison to the online 2DLC platform previously described, our system has several advantages including the use of a single switching valve (two including the injector) and two columns running at low flow rates (300 nL/min). Switching from capillary to nanoLC regimes is nontrivial because in order to minimize the dead times between each 2D separation the design of the connections and synchronization of the pump hardware need to be carefully optimized. Handling smaller volumes results in less dilution thus allowing for the reduction of the sample size from the 24 μg reported in ref 23 to 1.5 μg (roughly 20×). Moreover, the first separation (WCX-HILIC) runs throughout the entire analysis using a long and shallow gradient that allows for high resolution fractionation. The system is programmed so that all the second dimension gradients are performed by the time the first dimension is completed. The setup described by Tian et al.[23] collects 20 fractions from a 300 min WCX-HILIC separation, and each is analyzed using a 180 min RPLC gradient for a total of >60 h per analysis, while here each fraction was analyzed using a 13 min RPLC analysis resulting in 275 min per 2DLC analysis.

Additionally, we performed UVPD fragmentation to increase the confidence in histone proteoform identification.[19]

## Online Nanoflow LC×LC Using Active Modulation (2DLC)

In order to effectively couple two capillary based separations, it is important to minimize dead volumes in both LC dimensions and to ensure that the injection volume to the second dimension is sufficiently small to minimize cycle times and peak broadening.

For this reason, we substituted empty loops, typically used in LC×LC modulation interfaces ("passive modulation"), by capillary trap columns ("active modulation"). We previously described the principle of this approach in analytical[46] and low-flow[47] applications. These studies demonstrate how active modulation preserves the high LC separation power of online LC×LC and reduces sample dilution.

The nanoflow LC×LC setup combines a 150 mm × 75 μm ID WCX column separation at 200 nL/min, using a formic acid gradient from 70% ACN 1% FA to 68% ACN 8% FA, with a 100 mm × 50 μm ID C18 RPLC column separation at 300 nL/min using a water 0.1% FA to ACN 0.1% FA gradient. The ACN-rich eluent from the first dimension (strong eluting solvent in RPLC) is diluted 1:10 with water (1.6 μL/min) using a T-piece mixer. The eluent is loaded on 50 mm × 100 μm ID RPLC trap columns installed on a 10-port two-position nano HPLC valve. While a fraction eluting from the $^{1}$D is concentrated on a first trap, the second trap is used to inject a previously collected fraction onto the second-dimension column where a fast (10 min gradient time) separation takes place. The repetition of this process enables the sampling of several $^{1}$D fractions that are then simultaneously analyzed on the $^{2}$D. Using a low-dead volume switching valve (port to port volumes of 30 nL) and custom-made traps (with a mobile phase volume of about 250 nL) we were able to reduce the dead volume of the modulation unit to about 300 nL and complete $^{2}$D separations within a cycle time of 13 min (300 nL/min).

After the $^{1}$D gradient reached 100% B, we used the sampler injector to deliver solutions containing 8% FA and an increasing % of water to allow for elution of the most hydrophilic species retained on the $^{1}$D column, and thus ensure complete elution of proteins and other contaminants off the WCX column. Subsequently, we equilibrated the $^{1}$D column at a higher flow rate to prepare the column for the next injection. A schematic representation of the valve setup and gradient programming is depicted in Figure 2. Such an online nano 2DLC system represents the first of this kind, as the coupling of two nanoscale separation is a result of careful optimization of dead volumes, gradient delivery times, connection, and valve assembly to remove sources of air bubbles.

The nanoflow LC×LC setup eliminates sample losses typically associated with offline fractionation. Moreover, the nanoflow rates and small ID (50 μm) of the $^{2}$D column limits sample dilution during analysis. This allows injection of the



DOI: 10.1021/acs.jproteome.8b00458
J. Proteome Res. 2018, 17, 3791−3800

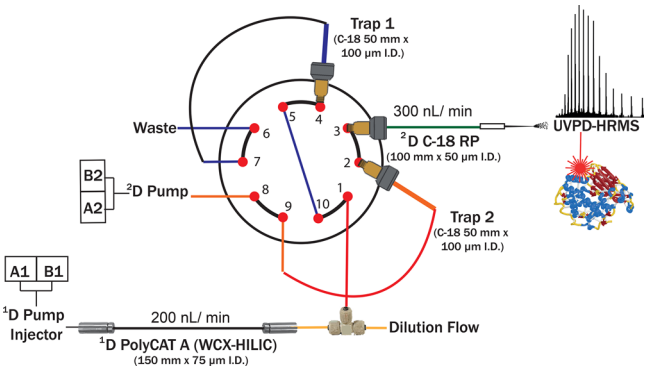


**Figure 2.** (a) Schematic representation of the 2DLC-MS/MS setup (WCX-HILIC/a×m/RPLC UVPD-HRMS). The sample components are separated using a gradient from 70% ACN 1%FA (A1) to 68% ACN 8% FA (B1; more details about the gradient programming are reported in the Experimental Section) on a WCX column, fractionated (online) using two trap columns (C18) and sequentially separated using a RPLC column (C18) with a water (A1) to ACN gradient (A2). During the analysis a dilution flow is delivered to reduce the elution strength of the mobile phase of the $^{1}$D (dilution flow rate ≈ 9× $^{1}$D flow rate) and allow the concentration of the analytes on a trap column (T1). Once the valve is switched, the analytes are eluted from the trap and separated on the $^{2}$D column. (b) Diagram reporting the gradient programmed for the $^{1}$D (WCX-HILIC) and $^{2}$D (RPLC); the green lines mark the injection events on the $^{1}$D column, while the blu and red trace the $^{1}$D and $^{2}$D gradient, respectively.

same quantity of protein as used in our RPLC and WCX-HILIC experiments (1.5 $\mu$g) without degrading sensitivity.

Figure 3a shows the 2DLC chromatogram of HeLa core histones aligned according to the $^{2}$D cycle time. Histone charge variants are separated by WCX-HILIC while RPLC separates histone families (H4 and H2B elute at the beginning of each RPLC analysis, followed by H2A and H3; the TIC of a single RPLC $^{2}$D run is reported in Figure S5 of the Supporting Information). Figure 3b overlays the TIC and LC-MS feature map, indicating the presence of the three histone families in most of the ($^{2}$D) RPLC separations.

Figure 4 shows H3 and H4 histone regions of the LC-MS feature map obtained with WCX-HILIC/a×m/RPLC. The distribution of masses over the WCX-HILIC retention window indicates that highly modified species elute early, following the separation trend that was observed when using WCX-HILIC alone. MS/MS analysis revealed that $^{1}$D histone proteoform separation is maintained and is mostly driven by the degree of acetylation; $^{2}$D further separates $^{1}$D fractions into different histone families.

Online WCX-HILIC/a×m/RPLC offers the advantage of coupling WCX to MS detection using RPLC mobile phases, allowing to preservative the separation selectivity of this technique but removing the high acid concentration used for elution in WCX (source of ion suppression). In addition, RPLC resolves histone proteoform fractions into families and compresses the (wide) peaks from WCX-HILIC (up to 10 min in some cases) to widths of less than 2 min for each RPLC analysis. This, in combination with the use of a 50-$\mu$m ID $^{2}$D column, increases the sensitivity of the technique, allowing detection of lower abundance proteoforms that would not be detected in a 1D WCX-HILIC MS experiment.

Triplicate analyses of HeLa core histones showed similar elution profiles as shown Supporting Material S5. The major source of variation appears to be the fractionation of the WCX-HILIC analysis in the first dimension in combination with potential degradation of the sample during the analysis process, which results in shifts in the concentrations present in the RPLC fraction.

To further compare the results obtained from one- and two-dimensional separations, we extracted deconvoluted mass features corresponding to the H2A/B, H3, and H4 proteoforms ($11200 < M_r < 11500$ for H4, $13650 < M_r < 14150$ for H2A/B, $15100 < M_r < 15500$ for H3) and then combined their masses into 1 Da bins (the results are plotted in Figure S6 of the Supporting Information, and the corresponding feature maps are in Supporting Material S3). This visualization of our data set removes the discrimination coming from the retention time and thus the distinction of isobaric compounds but represents a simple method to compare the MS1 features detected. From this comparison we observed that more MS features not detected by 1D WCX or RPLC alone are observed in 2DLC experiments, especially for H3 histones (H4:66 nLC×LC, 54 WCX-HILIC, 65 RPLC; H2A/B 125 nLC×LC, 59 WCX, 99 RPLC and H3:160 nLC×LC, 67 WCX, 62 RPLC). It is likely that part of the MS features not detected either by WCX or RPLC are due to proteoform coelution and consequent ion suppression.

## Proteoform Identification

The workflow used in this study included high resolution MS1 (120 000 at $m/z$ = 200) followed by isolation of the five most abundant precursor ions for subsequent UVPD fragmentation (an illustration of the identification process is reported in Figure S1 of the Supporting Information). Similar to the approach described by Tian et al.,[28,42] we initially searched MS/MS data against a database containing histones and major protein contaminants (the complete list is reported in Table S2 of the Supporting Information). In Table 2 we report the results for the 1D RPLC, 1D WCX-HILIC and LC×LC WCX-HILIC/a×m/RPLC analyses using Prosight PC.

A direct comparison of the identification results published using other offline and online 2DLC approaches (Tian[28,42]) is not possible, as the data were produced using different fragmentation approaches on a different mass spectrometer and data processing. We refer to Greer et al.[19] for a comparison of the results of online RPLC with UVPD fragmentation with respect to HCD and EThcD.

The number of identifications reported (1D and 2DLC) may appear lower relative to what has been reported for other histone top-down studies.[28] This is likely due to the tighter tolerances for precursor and fragment ions (10 ppm vs 1 to 10 Da reported previously[8,28]). Analyses using relaxed parameters to increase the number of proteoforms identified, but we preferred using restrictive matching settings to increase the confidence in the data presented.

Using WCX and WCX-HILIC/a×m/RPLC we predominantly identified intact proteoforms while RPLC predominantly identified truncated proteoforms. The shallow gradient and long column used in RPLC-MS allow the truncated forms (lower in abundance) to be resolved from their intact proteins and elute throughout the analysis. In contrast, in WCX-HILIC the truncated forms elute only in the initial part of the run and are less likely to be resolved and identified. The same phenomena happen in the 2DLC setup; additionally, the fast gradient used in the second-dimension chromatography reduces the number of truncated forms that are observable.



DOI: 10.1021/acs.jproteome.8b00458
J. Proteome Res. 2018, 17, 3791−3800

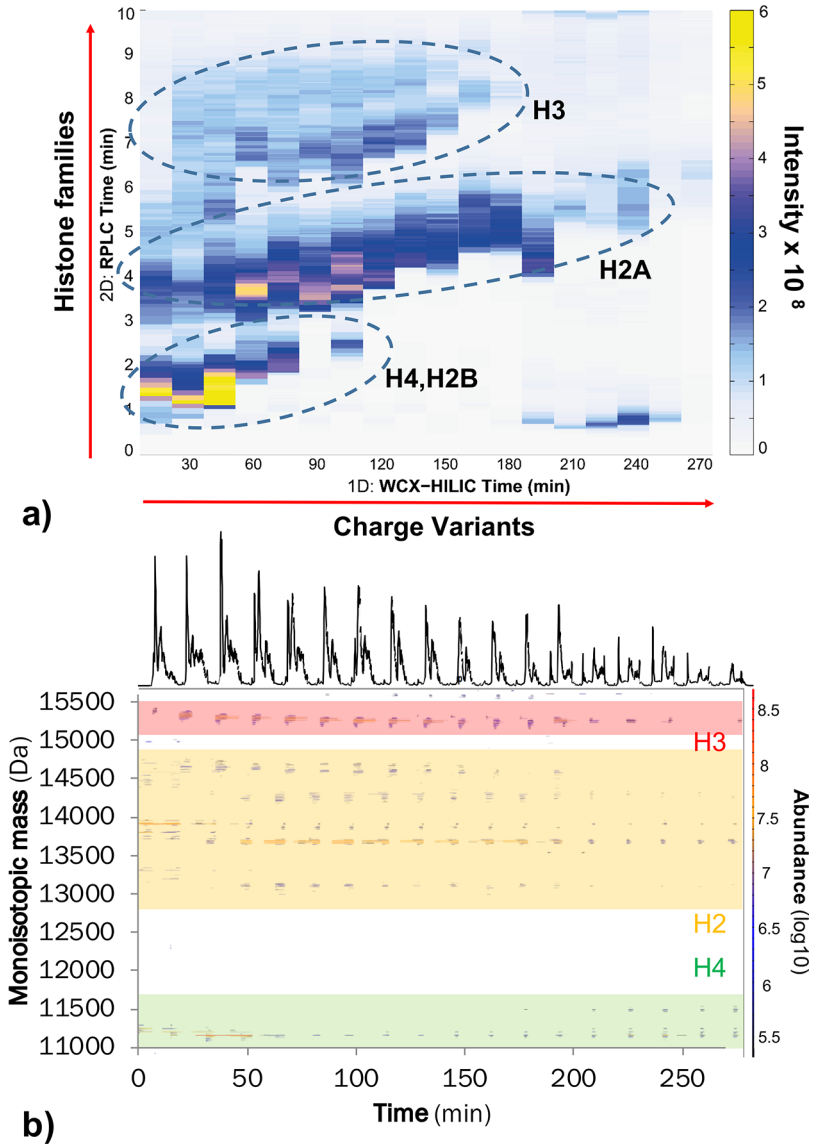


**Figure 3.** WCX-HILIC/a×m/RPLC UVPD-HRMS analysis of HeLa core histones. (a) Folded 2D chromatogram extracted from the total ion chromatograms (TICs). 2DLC separation combines the charge resolving power from the WCX separation with the histone family group separation (H2, H3, H4) afforded by RPLC. (b) TICs (top) of the 2DLC separation and the respective neutral mass spectra (bottom).

RPLC-MS analysis yielded a higher number of H2A and H2B proteoforms, whereas WCX identified a significantly larger number of H3 proteoforms. Notably, the 2DLC setup combines the specificity of both the separations, allowing for the identification of more proteins for all family groups. These results can be explained by the configuration of our 2DLC setup where the $^{1}$D (WCX-HILIC) separates protein charge variants using a long and shallow gradient that is fractionated at an interval of 13 min; fractions are sequentially injected on $^{2}$D (RPLC) for protein family separations. The mass distribution for the identified proteoforms (Figure S6 of the Supporting Information), as well as the feature maps shown in Supporting Material S3, indicate that methods based on ion exchange (WCX-HILIC and 2DLC) are particularly well suited to resolve H3 forms. For targeted analysis of H2 and/or H4 using the 2DLC platform, it may be necessary to further optimize both separation dimensions. However, 1D RPLC separations, employing long columns and shallow gradients, would likely provide better separation of H2A and H2B proteoforms, which differ slightly in their primary amino acid sequence.[42]

Overall, WCX-HILIC/a×m/RPLC identified more proteoforms in comparison to both 1D approaches. The combination of independent chemically selective separations reduces ion suppression and provides an increased dynamic range of measurements proving the usefulness of such a separation strategy. We speculate that increasing the column length in the first-dimension column and allowing for a longer analysis time and higher sample injection amount would further increase the separation capacity and possibly the data quality obtained.

To further evaluate our results, we performed only absolute mass ProSight searches against the entire human protein database. Analyses with a narrow search window for precursor and fragment ions (10 ppm) were completed in less than 30 min per data set. We used the *C* score parameter to evaluate the results. This metric measures the level of characterization of a proteoform using a Bayesian approach.[31] For instance, a *C* score of 3 indicates that two proteoforms in the database can



DOI: 10.1021/acs.jproteome.8b00458
*J. Proteome Res.* 2018, 17, 3791−3800

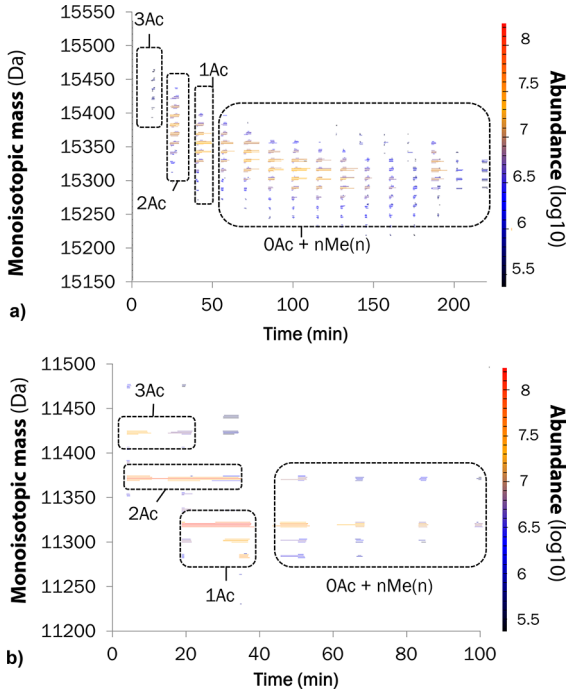


**Figure 4.** Detailed view extracted from Figure 3 showing the neutral mass region of H3 (a) and H4 (b) histones. Species with a higher degree of acetylation (Ac) (i.e., with higher molecular mass) have lower retention in WCX-HILIC. Information on histone identifications is provided in Supporting Material S6.

equally well explain the observed data (different combination of PTM), and proteoforms with *C* scores of 40 or higher are considered to be unambiguously identified. Table 2 shows the distribution of the identification with a *C* score below 3 (IDs that can be connected with multiple proteoforms), between 3 and 45 (IDs with up to 2 proteoforms), and more than 45 (unique proteoforms).

An absolute mass ProSight search halved the number of unique histone proteoforms identified relative to searches using a restricted database (Table 1), suggesting that a large number of identified proteoforms had not been explicitly included in the annotated database.

The proteoforms identified included several acetylated, (tri-, di-, mono-) methylated, and phosphorylated histone groups. The overlap between identifications (*C* score >3) obtained using different separation approaches is depicted in Figure 5.

The results of this analysis show a large overlap between the identifications from the three techniques employed, with more than 70% of all the identifications being generated from the WCX-HILIC/a×m/RPLC analyses. Finally, the overlap between the proteoforms identified in triplicate analyses (and processed using the same data analysis workflow) accounted for about 40% for WCX-HILIC/a×m/RPLC. The main source of variability between identified proteoforms is the large diversity of H3 proteoforms. This histone family displays a large diversity in the type and location of PTMs, and our results suggest that each analysis may capture only part of this great complexity. Despite improvements in the separation of intact histones enabled by 2DLC, several proteoforms share the same mass coelute. Thus, the quantitative analysis of the data presented can only be attempted monitoring characteristic fragment intensities and requires the development of specific software[48] and was not attempted in our study.

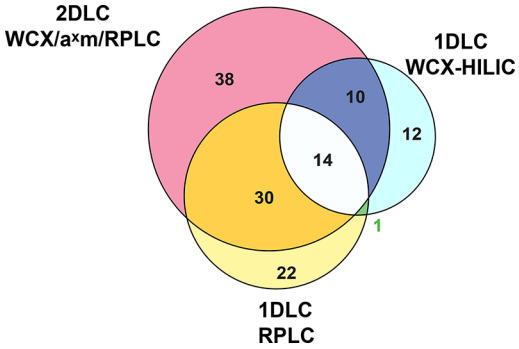


**Figure 5.** Venn diagram of the histone proteoforms identified with *C* > 3 using 1DLC RPLC-MS, 1DLC WCX-HILIC-MS, and 2DLC WCX-HILIC/a×m/RPLC-MS (3); Protein IDs available in Table S4 of the Supporting Information.

## CONCLUSIONS

The vast heterogeneity of histone proteins makes them challenging analytes for top-down MS investigations. This complexity stems from several sources: positional isomers (i.e., different PTM site on the same proteoform), small mass differences between PTMs (e.g., acetylation and trimethylation), and the presence of unknown/unexpected PTMs (e.g., bromination[42]).

Our results demonstrate the high potential of an online nanoflow 2DLC separation for top-down proteomic analyses of histone proteoforms. The separation strength of the proposed method lays in the combination of the chemical selectivity of two orthogonal separation modalities. Herein, the two methods are coupled online to reduce sample losses typical for offline fractionation schemes. In addition, nanoflows were used to reduce sample dilution and enhance MS sensitivity. Ultimately, the combined advantages of this platform allow for the extension of the dynamic range of the MS measurement, increasing the number of confidently identified histone proteoforms relative to 1DLC-MS.

## ASSOCIATED CONTENT

### Supporting Information

The Supporting Information is available free of charge on the ACS Publications website at DOI: 10.1021/acs.jproteome.8b00458.

Gradient programming of the 2DLC (Supporting Material S1, Table S1), a schematic illustration of the histone identification workflow (Supporting Material S2, Figure S1). Additional data on 1DLC and 2DLC separations are reported in the Supporting Material S3. This include details of the separation families by 1DLC WCX-HILIC (Figure S2), 1DLC RPLC (Figure S3), 2DLC WCX-HILIC/a×m/RPLC (Figure S4), the TIC of a single modulation of the 2DLC separation (Figure S5), and the analysis of the distribution of neutral masses detected for each histone family (Figure S6). The list of families of proteins identified using WCX-HILIC/a×m/RPLC UVPD-HRMS (Prosight PC 4.0) is collected in Supporting Material S4, Table S2. The results from the triplicate analysis of HeLa Histones using the WCX-HILIC/a×m/RPLC UVPD-HRMS platform are in the Supporting Material S5, Figure S7. In Supporting Materials S6 and S7 are reported examples of proteoform IDs obtained with our analysis



DOI: 10.1021/acs.jproteome.8b00458
J. Proteome Res. 2018, 17, 3791−3800

workflow using respectively the informed proteomics and Prosight PC data analysis toolkit. Figure S8 shows a detail of Figure 2 reporting the monoisotopic mass area of H3 histones and assignment of H3.2 proteoforms using the informed proteomics workflow and Figure S9–S14 examples of H3.2 proteoform IDs. Figure S15 shows a detail of Figure 2 reporting the monoisotopic mass area of H4 histones and assignment of H4 proteoforms using the informed proteomics workflow and Figure S16–S19 examples of H4 proteoform IDs. Examples of sequence coverage of protein identifications using Prosight PC 4.0 are collected in Supporting Material S7 (PDF)

Excel file reporting the output of the Prosight PC 4.0 searches summarized in Table S3 (list of proteoform identified by Prosight PC 4.0 using a restricted database) (XLSX)

Excel file reporting the output of the Prosight PC 4.0 searches summarized in Table S4 (list of proteoforms identified using Prosight PC 4.0 using the Human Proteome database and filtered by *C* score) (XLSX)

## AUTHOR INFORMATION


### Corresponding Author

*E-mail: a.gargano@uva.nl. Tel: +31-20-525 7040.

### ORCID

Andrea F. G. Gargano: 0000-0003-3361-7341
Jared B. Shaw: 0000-0002-1130-1728
Mowei Zhou: 0000-0003-3575-3224


### Notes

The authors declare no competing financial interest.

## ACKNOWLEDGMENTS

This work was financially supported by The Netherlands Organization for Scientific Research by the NWO Veni grant IPA (722.015.009). The authors would like to thank Nikola Tolic and Rui Zhao from the Pacific Northwest National Laboratories as well as Andrei Barcaru and Eva M.O.L. Johansson from the University of Amsterdam for their support and valuable discussions. We gratefully acknowledge Dr. Andrew Alpert (PolyLC inc.) for the support in developing the WCX-HILIC method and Hagen Preik-Steinhoff (VICI-Valco) for the kind gift of the nano HPLC valve. This work was performed at EMSL, a national scientific user facility sponsored by the Office of Biological and Environmental Research, U.S. Department of Energy (DOE). EMSL is located at PNNL, a multidisciplinary national laboratory operated by Battelle for the U.S. DOE.

## REFERENCES


(1) Huang, H.; Lin, S.; Garcia, B. A.; Zhao, Y. Quantitative proteomic analysis of histone modifications. *Chem. Rev.* **2015**, *115* (6), 2376–2418.

(2) Strahl, B. D.; Allis, C. D. The language of covalent histone modifications. *Nature* **2000**, *403* (6765), 41–45.

(3) Jenuwein, T.; Allis, C. D. Translating the histone code. *Science (Washington, DC, U. S.)* **2001**, *293* (5532), 1074–1080.

(4) Wang, Z.; Zang, C.; Rosenfeld, J. A.; Schones, D. E.; Barski, A.; Cuddapah, S.; Cui, K.; Roh, T. Y.; Peng, W.; Zhang, M. Q.; et al. Combinatorial patterns of histone acetylations and methylations in the human genome. *Nat. Genet.* **2008**, *40* (7), 897–903.

(5) Karch, K. R.; Sidoli, S.; Garcia, B. A. *Chapter One – Identification and Quantification of Histone PTMs Using High-Resolution Mass Spectrometry*, 1st ed.; Elsevier Inc.: 2016; Vol. *574*.

(6) Peach, S. E.; Rudomin, E. L.; Udeshi, N. D.; Carr, S. A.; Jaffe, J. D. Quantitative Assessment of Chromatin Immunoprecipitation Grade Antibodies Directed against Histone Modifications Reveals Patterns of Co-occurring Marks on Histone Protein Molecules. *Mol. Cell. Proteomics* **2012**, *11* (5), 128–137.

(7) Contrepois, K.; Ezan, E.; Mann, C.; Fenaille, F. Ultra-high performance liquid chromatography-mass spectrometry for the fast profiling of histone post-translational modifications. *J. Proteome Res.* **2010**, *9* (10), 5501–5509.

(8) Liu, X.; Hengel, S.; Wu, S.; Tolic, N.; Pasa-Tolic, L.; Pevzner, P. A. Identification of ultramodified proteins using top-down tandem mass spectra. *J. Proteome Res.* **2013**, *12* (12), 5830–5838.

(9) Baker, M. Mass spectrometry for chromatin biology. *Nat. Methods* **2012**, *9* (7), 649–652.

(10) Garcia, B. A.; Mollah, S.; Ueberheide, B. M.; Busby, S. A.; Muratore, T. L.; Shabanowitz, J.; Hunt, D. F. Chemical derivatization of histones for facilitated analysis by mass spectrometry. *Nat. Protoc.* **2007**, *2* (4), 933–938.

(11) Yuan, Z.-F.; Arnaudo, A. M.; Garcia, B. a. Mass spectrometric analysis of histone proteoforms. *Annu. Rev. Anal. Chem.* **2014**, *7*, 113–128.

(12) Britton, L.-M. P.; Gonzales-Cope, M.; Zee, B. M.; Garcia, B. A. Breaking the histone code with quantitative mass spectrometry. *Expert Rev. Proteomics* **2011**, *8* (5), 631–643.

(13) Smith, L. M.; Kelleher, N. L. Proteoform: a single term describing protein complexity. *Nat. Methods* **2013**, *10* (3), 186–187.

(14) Maile, T. M.; Izrael-Tomasevic, A.; Cheung, T.; Guler, G. D.; Tindell, C.; Masselot, A.; Liang, J.; Zhao, F.; Trojer, P.; Classon, M.; et al. Mass Spectrometric Quantification of Histone Post-translational Modifications by a Hybrid Chemical Labeling Method. *Mol. Cell. Proteomics* **2015**, *14* (4), 1148–1158.

(15) Zheng, Y.; Huang, X.; Kelleher, N. L. Epiproteomics: Quantitative analysis of histone marks and codes by mass spectrometry. *Curr. Opin. Chem. Biol.* **2016**, *33*, 142–150.

(16) Molden, R. C.; Garcia, B. A. Middle-down and top-down mass spectrometric analysis of co-occurring histone modifications. *Curr. Protoc. Protein Sci.* **2014**, *77* (1), 23.7.1–23.7.28.

(17) Tvardovskiy, A.; Wrzesinski, K.; Sidoli, S.; Fey, S. J.; Rogowska-Wrzesinska, A.; Jensen, O. N. Top-down and Middle-down Protein Analysis Reveals that Intact and Clipped Human Histones Differ in Post-translational Modification Patterns. *Mol. Cell. Proteomics* **2015**, *14* (12), 3142–3153.

(18) Azad, G. K.; Tomar, R. S. Proteolytic clipping of histone tails: The emerging role of histone proteases in regulation of various biological processes. *Mol. Biol. Rep.* **2014**, *41* (5), 2717–2730.

(19) Greer, S. M.; Brodbelt, J. S. Top-Down Characterization of Heavily Modified Histones Using 193 nm Ultraviolet Photodissociation Mass Spectrometry. *J. Proteome Res.* **2018**, *17* (3), 1138–1145.

(20) Wang, T.; Holt, M. V.; Young, N. L. The histone H4 proteoform dynamics in response to SUV4–20 inhibition reveals single molecule mechanisms of inhibitor resistance. *Epigenet. Chromatin* **2018**, *11* (1), 1–18.

(21) Dang, X.; Singh, A.; Spetman, B. D.; Nolan, K. D.; Isaacs, J. S.; Dennis, J. H.; Dalton, S.; Marshall, A. G.; Young, N. L. Label-Free Relative Quantitation of Isobaric and Isomeric Human Histone H2A and H2B Variants by Fourier Transform Ion Cyclotron Resonance Top-Down MS/MS. *J. Proteome Res.* **2016**, *15* (9), 3196–3203.

(22) Toby, T. K.; Fornelli, L.; Kelleher, N. L. Progress in Top-Down Proteomics and the Analysis of Proteoforms. *Annu. Rev. Anal. Chem.* **2016**, *9* (1), 499–519.

(23) Tian, Z.; Zhao, R.; Tolić, N.; Moore, R. J.; Stenoien, D. L.; Robinson, E. W.; Smith, R. D.; Paša-Tolić, L. Two-dimensional liquid chromatography system for online top-down mass spectrometry. *Proteomics* **2010**, *10* (20), 3610–3620.




DOI: 10.1021/acs.jproteome.8b00458
*J. Proteome Res.* 2018, 17, 3791–3800

(24) Zhou, M.; Wu, S.; Stenoien, D. L.; Zhang, Z.; Connolly, L.; Freitag, M.; Pasa-Tolic, L. Profiling changes in histone post-translational modifications by top-down mass spectrometry. In *Methods Mol. Biol.*; 2017; Vol. *1507*, pp 153−168.
(25) Shaw, J. B.; Li, W.; Holden, D. D.; Zhang, Y.; Griep-Raming, J.; Fellers, R. T.; Early, B. P.; Thomas, P. M.; Kelleher, N. L.; Brodbelt, J. S. Complete protein characterization using top-down mass spectrometry and ultraviolet photodissociation. *J. Am. Chem. Soc.* **2013**, *135* (34), 12646−12651.
(26) Cannon, J. R.; Holden, D. D.; Brodbelt, J. S. Hybridizing ultraviolet photodissociation with electron transfer dissociation for intact protein characterization. *Anal. Chem.* **2014**, *86* (21), 10970−10977.
(27) Cleland, T. P.; DeHart, C. J.; Fellers, R. T.; Vannispen, A. J.; Greer, J. B.; LeDuc, R. D.; Parker, W. R.; Thomas, P. M.; Kelleher, N. L.; Brodbelt, J. S. High-Throughput Analysis of Intact Human Proteins Using UVPD and HCD on an Orbitrap Mass Spectrometer. *J. Proteome Res.* **2017**, *16* (5), 2072−2079.
(28) Tian, Z.; Tolić, N.; Zhao, R.; Moore, R. J.; Hengel, S. M.; Robinson, E. W.; Stenoien, D. L.; Wu, S.; Smith, R. D.; Paša-Tolić, L.; et al. Enhanced top-down characterization of histone post-translational modifications. *Genome Biol.* **2012**, *13* (10), R86.
(29) Fort, K. L.; Dyachenko, A.; Potel, C. M.; Corradini, E.; Marino, F.; Barendregt, A.; Makarov, A. A.; Scheltema, R. A.; Heck, A. J. R. Implementation of Ultraviolet Photodissociation on a Benchtop Q Exactive Mass Spectrometer and Its Application to Phosphoproteomics. *Anal. Chem.* **2016**, *88* (4), 2303−2310.
(30) Park, J.; Piehowski, P. D.; Wilkins, C.; Zhou, M.; Mendoza, J.; Fujimoto, G. M.; Gibbons, B. C.; Shaw, J. B.; Shen, Y.; Shukla, A. K.; et al. Informed-Proteomics: Open-source software package for top-down proteomics. *Nat. Methods* **2017**, *14* (9), 909−914.
(31) Leduc, R. D.; Fellers, R. T.; Early, B. P.; Greer, J. B.; Thomas, P. M.; Kelleher, N. L. The C-Score: A bayesian framework to sharply improve proteoform scoring in high-throughput top down proteomics. *J. Proteome Res.* **2014**, *13* (7), 3231−3240.
(32) Lindner, H.; Sarg, B.; Meraner, C.; Helliger, W. Separation of acetylated core histones by hydrophilic-interaction liquid chromatography. *J. Chromatogr. A* **1996**, *743* (1), 137−144.
(33) Lindner, H.; Sarg, B.; Helliger, W. Application of hydrophilic-interaction liquid chromatography to the separation of phosphorylated H1 histones. *J. Chromatogr. A* **1997**, *782* (1), 55−62.
(34) Benevento, M.; Tonge, P. D.; Puri, M. C.; Nagy, A.; Heck, A. J. R.; Munoz, J. Fluctuations in histone H4 isoforms during cellular reprogramming monitored by middle-down proteomics. *Proteomics* **2015**, *15* (18), 3219−3231.
(35) Young, N. L.; DiMaggio, P. a.; Plazas-Mayorca, M. D.; Baliban, R. C.; Floudas, C. A.; Garcia, B. A. High throughput characterization of combinatorial histone codes. *Mol. Cell. Proteomics* **2009**, *8* (10), 2266−2284.
(36) Jung, H. R.; Sidoli, S.; Haldbo, S.; Sprenger, R. R.; Schwämmle, V.; Pasini, D.; Helin, K.; Jensen, O. N. Precision mapping of coexisting modifications in histone H3 tails from embryonic stem cells by ETD-MS/MS. *Anal. Chem.* **2013**, *85* (17), 8232−8239.
(37) Mizzen, C. A.; Alpert, A. J.; Lévesque, L.; Kruck, T. P. A.; McLachlan, D. R. Resolution of allelic and non-allelic variants of histone H1 by cation-exchange-hydrophilic-interaction chromatography. *J. Chromatogr., Biomed. Appl.* **2000**, *744* (1), 33−46.
(38) Papazyan, R.; Taverna, S. D. Separation and Purification of Multiply Acetylated Proteins Using Cation-Exchange Chromatography. *Methods Mol. Biol.* **2013**, *981*, 103−113.
(39) Lindner, H. H. Analysis of histones, histone variants, and their post-translationally modified forms. *Electrophoresis* **2008**, *29* (12), 2516−2532.
(40) Zheng, Y.; Fornelli, L.; Compton, P. D.; Sharma, S.; Canterbury, J.; Mullen, C.; Zabrouskov, V.; Fellers, R. T.; Thomas, P. M.; Licht, J. D.; et al. Unabridged Analysis of Human Histone H3 by Differential Top-Down Mass Spectrometry Reveals Hypermethylated Proteoforms from MMSET/NSD2 Overexpression. *Mol. Cell. Proteomics* **2016**, *16* (18), 1−40.
(41) Garcia, B. A.; Thomas, C. E.; Kelleher, N. L.; Mizzen, C. A. Tissue-specific expression and post-translational modification of histone H3 variants. *J. Proteome Res.* **2008**, *7* (10), 4225−4236.
(42) Zhou, M.; Paša-Tolić, L.; Stenoien, D. L. Profiling of Histone Post-Translational Modifications in Mouse Brain with High-Resolution Top-Down Mass Spectrometry. *J. Proteome Res.* **2017**, *16* (2), 599−608.
(43) Su, X.; Jacob, N. K.; Amunugama, R.; Lucas, D. M.; Knapp, A. R.; Ren, C.; Davis, M. E.; Marcucci, G.; Parthun, M. R.; Byrd, J. C.; et al. Liquid chromatography mass spectrometry profiling of histones. *J. Chromatogr. B: Anal. Technol. Biomed. Life Sci.* **2007**, *850* (1−2), 440−454.
(44) Giddings, J. C. C. Sample dimensionality: A predictor of order-disorder in component peak distribution in multidimensional separation. *J. Chromatogr. A* **1995**, *703* (1−2), 3−15.
(45) Pesavento, J. J.; Bullock, C. R.; LeDuc, R. D.; Mizzen, C. A.; Kelleher, N. L. Combinatorial modification of human histone H4 quantitated by two-dimensional liquid chromatography coupled with top down mass spectrometry. *J. Biol. Chem.* **2008**, *283* (22), 14927−14937.
(46) Gargano, A. F. G.; Duffin, M.; Navarro, P.; Schoenmakers, P. J. Reducing Dilution and Analysis Time in Online Comprehensive Two-Dimensional Liquid Chromatography by Active Modulation. *Anal. Chem.* **2016**, *1*, 1−16.
(47) Vonk, R. J.; Gargano, A. F. G.; Davydova, E.; Dekker, H. L.; Eeltink, S.; de Koning, L. J.; Schoenmakers, P. J. Comprehensive Two-Dimensional Liquid Chromatography with Stationary-Phase-Assisted Modulation Coupled to High-Resolution Mass Spectrometry Applied to Proteome Analysis of Saccharomyces cerevisiae. *Anal. Chem.* **2015**, *87* (10), 5387−5394.
(48) Yuan, Z. F.; Sidoli, S.; Marchione, D. M.; Simithy, J.; Janssen, K. A.; Szurgot, M. R.; Garcia, B. A. EpiProfile 2.0: A Computational Platform for Processing Epi-Proteomics Mass Spectrometry Data. *J. Proteome Res.* **2018**, *17* (7), 2533−2541.


DOI: 10.1021/acs.jproteome.8b00458
*J. Proteome Res.* 2018, 17, 3791−3800